Journal of Food Engineering 313 (2022) 110750

Contents lists available at ScienceDirect

Journal of Food Engineering

journal homepage: www.elsevier.com/locate/jfoodeng

An experimental protocol to determine quality parameters of dry-cured loins using low-field Magnetic Resonance Imaging

Daniel Caballero [a,b,*], Pablo G. Rodríguez [b], Andrés Caro [b], María del Mar Ávila [b], Juan P. Torres [b], Teresa Antequera [c], Trinidad Perez-Palacios [c]

[a] Chemometrics and Analytical Technology, Food Technology Department, Faculty of Science, University of Copenhagen, Rolighedsvej, 26, DK-1958, Frederiksberg C, Denmark

[b] Media Engineering Group, Research Institute of Meat and Meat Products, University of Extremadura, Avda. Ciencias S/N, ES-10.003, Cáceres, Spain

[c] Food Technology Department, Research Institute of Meat and Meat Products, University of Extremadura, Avda. Ciencias S/N, ES-10.003, Cáceres, Spain

ARTICLE INFO

Keywords:
Experimental protocol
Magnetic resonance imaging
Optimum procedures
Dry-cured loins
Quality parameters

ABSTRACT

The objective of this study was to achieve an experimental protocol (EP) to determine quality characteristics of dry-cured loins non-destructively by using low-field (LF) Magnetic Resonance Imaging (MRI). The MRI procedure is composed of three main stages: MRI acquisition, MRI analysis (computer vision techniques) and data analysis (data mining methods). Two procedures have been implemented within a EP and validated with real samples from the meat industry (dry-cured loins, n = 100) by means of different quality measures. The validation results may indicate the use of both implemented procedures and the development of an EP to determine quality characteristics of loins by LF MRI-computer vision-data mining in a non-destructive way, with high accuracy and reducing the dispersion of the values. This brings the possibility of implementing this methodology in meat processing plants.

1. Introduction

The evaluation of quality characteristics of meat and meat products are usually carried out by means of tedious and time and solvent consuming methods that usually involve the destruction of the samples. In this sense, the use of non-destructive techniques, such as computed tomography (CT) (Picouet et al., 2013; Vestergaard et al., 2015), near infrared spectroscopy (NIRs) (González-Mohino et al., 2018; Pérez-Palacios et al., 2019) or Magnetic Resonance Imaging (MRI) have been proposed as alternative-complementary techniques.

Among them, MRI has a set of characteristics (non-destructive, non-invasive, non-intrusive, innocuous and taking information from the inner of the solid samples) that make it be so appropriate for the food analysis, though CT is ionizing, and minced samples are preferred when using NIRs (Caballero et al., 2021). In fact, several studies have been focused on the evaluation of the use of MRI to analyse meat and meat products. These works have been principally carried out using high field (HF) MRI scanners, which have a magnetic field higher than 2 T, giving very high-quality images. However, these devices are very expensive and require high maintenance costs (Feig, 2011; Ladd et al., 2018). Most studies by HF MRI scanners have analysed hams, there also being some publications on beef, pork and lamb samples (Caballero et al., 2021).

The methodology applied in these HF MRI studies for analysing meat and meat products differs in the acquisition sequences, the algorithms to

Abbreviations: CT, Computed Tomography; NIRs, Near Infrared Spectroscopy; MRI, Magnetic Resonance Imaging; HF, High Field; LF, Low Field; EP, Experimental protocol; GE, Gradient Echo; SE, Spin Echo; T3D, Turbo 3D; FOV, Field of view; TE, Echo time; TR, Repetition time; GLCM, Gray Level Co-occurrence Matrix; OPFTA, One Point of Fractal Texture Analysis; ROI, Region of Interest; ENE, Energy; ENT, Entropy; COR, Correlation; HC, Haralick's Correlation; IDM, Inverse Difference Moment; INE, Inertia; CS, Cluster Shade; CP, Cluster Prominence; CON, Contrast; DIS, Dissimilarity; UNI, Uniformity; HOM, Homogeneity; EFI, Efficiency; MLR, Multiple Linear Regression; KDD, Knowledge Discovery in Databases; WEKA, Waikato Environment for Knowledge Analysis; R, Correlation coefficient; MAE, Mean Absolute Error; RMSE, Root Mean Square Error; TSTD, True Standard Deviation; WAPE, Weighted Absolute Percentage Error; RF, Radiofrequency; GLRLM, Gray Level Run Length Matrix; NGLDM, Neighbouring Gray Level Dependence Matrix; CFA, Classical Fractal Algorithm; FTA, Fractal Texture Algorithm; IR, Isotonic Regression.

* Corresponding author. Chemometrics and Analytical Technology, Food Technology Department, Faculty of Science, University of Copenhagen, Rolighedsvej, 26, DK-1958, Frederiksberg C, Denmark.

E-mail address: dcaballero@unex.es (D. Caballero).

https://doi.org/10.1016/j.jfoodeng.2021.110750
Received 7 April 2021; Received in revised form 20 July 2021; Accepted 22 July 2021
Available online 29 July 2021

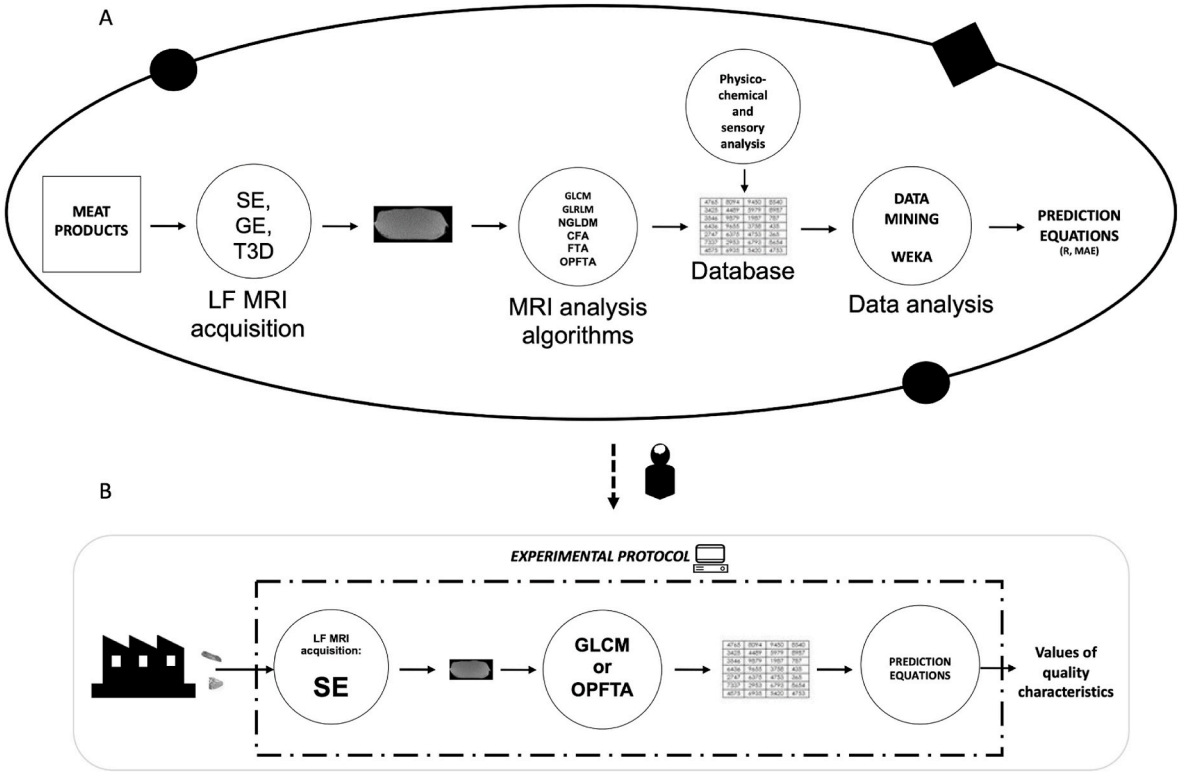

Fig. 1. Implementation (A) of the experimental protocol (B) evaluated in the present study.

analyse the image as well as on the data analysis technique. Main purposes of these works were to monitor the processing or cooking of the products, to classify different samples and to predict their quality characteristics. Accurate results have been shown in most cases.

Nowadays, the use of low field (LF) MRI scanners is increasing, with some recent publication on pork samples and dry-cured hams (Bernau et al., 2015; Torres et al., 2019). These scanners have a lower cost than HF ones and do not have maintenance costs. They generate magnetic field between 0.15 and 0.50 T (Ladd et al., 2018), and, consequently, the obtained images are of lower quality than those from HF MRI scanners. This aspect supposes a challenge to obtain an accurate analysis of the products and requires the optimization of the methodology, specially the procedures for the acquisition and analysis of the images. In fact, the activity of our research group in the last years have aimed to establish the optimum procedures for the LF MRI acquisition, the image analysis and the data analysis, to determine the quality characteristics of pork loins non-destructively (Ávila et al., 2018; Caballero et al., 2018a,b).

Nevertheless, despite the number of studies on MRI to analyse meat and meat products in a non-destructive way, there is no data about the development of any experimental protocol (EP) based on MRI, which can be applied for industrial use.

Considering all these aspects, the present study aimed to take a step forward by implementing the optimum procedure of LF MRI – computational analysis into an EP and evaluating its efficiency at industrial level.

2. Material and methods

2.1. Experimental design

The experimental design of the present work is composed of two parts. The first one dealt to compare the capability of the different techniques previously applied (for the image acquisition, image analysis and data analysis) to predict quality parameters of pork loins (Caballero et al., 2017a,b; 2018a,b; Pérez-Palacios et al., 2017). This comparison led to the optimum combinations of techniques, which were selected to get the EP (Fig. 1). The EP was operationalized within the official analysis service for meat and meat products ("Animal Source Foodstuffs Innovation Services" or "SiPA") of the Faculty of Veterinary Science at University of Extremadura (Cáceres, Spain). Thus, the second experiment consisted on evaluating the accuracy of the proposed EP with real samples (dry-cured loins, n = 100) from the meat industry. For that, the samples were first analysed using the proposed EP, obtaining "predicted" values of physico-chemical and sensory characteristics. These samples were also analysed by means of physico-chemical and sensory methods to verify the predicted values.

2.2. Experimental protocol

The EP implemented in this study takes three consecutive stages: image acquisition, image analysis and application of prediction equations.

2.2.1. Image acquisition

MRI images are acquired using a LF MRI scanner (ESAOTE VET-MR E-SCAN XQ 0.18 T) with a hand/wrist coil, applying T1-weighted sequences of Spin Echo (SE). The acquisition sequence influenced significantly on the values of the computational features and, also on the prediction results. Overall, the highest correlation coefficients were achieved when using SE, followed by Gradient Echo (GE), and Turbo 3D (T3D) having the lowest values (Caballero et al., 2017a,b; 2018a,b). These effects have been ascribed to the low bandwidth and high signal to noise ratio of SE. Consequently, SE has been chosen as the acquisition sequence for the EP. In fact, most of the MRI studies on meat and meat products have applied SE (Pérez-Palacios et al., 2010a,b).

For the acquisition sequence with SE, the following parameters were used: Field of view (FOV): 150 × 150 mm^2, echo time (TE): 26 ms, slice thickness: 4 mm, flip angle: 90°, repetition time (TR): 630 ms, matrix size: 256 × 204, phase encode: 204, number of acquisitions: five per sample. Twenty-nine slices per sample were obtained and the MRI

acquisition took 50 min for each sample. The MRI acquisition was performed at 23 °C. All images were acquired in DICOM format with 512 × 512 resolution and 256 Gy levels.

2.2.2. Image analysis

The MRI images can be analysed by means of computer vision algorithms, to extract numerical features from the images. Algorithms based on textures (GLCM, GLRLM (Gray Level Run Length Matrix) and NGLDM (Neighbouring Gray Level Dependence Matrix)) and fractals (CFA (Classical Fractal Algorithm), FTA (Fractal Texture Algorithm) and OPFTA) have been tested to analyse the MRI images of pork loins (Caballero et al., 2018a). One algorithm based on textures (Gray Level Co-occurrence Matrix (GLCM)) and other on fractals (One Point Fractal Texture Algorithm (OPFTA)) were chosen for this EP.

2.2.2.1. Gray level CO-OCCURRENCE matrix. Firstly, the largest area rectangle inscribed in the contour of the loin muscle is selected (Molano et al., 2012). This is called region of interest (ROI), which is finally analysed by GLCM. GLCM (Haralick et al., 1973; Haralick and Shapiro, 1993) was computed by counting the number of times that each pair of gray levels occurred at a given distance "*d*" in all directions. In this matrix, each item *p(i, j)* denotes the number of times that two neighbouring pixels separated by distance ($d = 1$ in this case) occur on the image, one with gray level *"i"* and the other with gray level *"j"*, in all 2D directions: 0°, 45°, 90°, 135°. These co-occurrences are accumulated into a single matrix, from which all the textural features are extracted. Ten computational texture features were obtained from this method proposed by Haralick et al. (1973): energy (ENE), entropy (ENT), correlation (COR), haralick's correlation (HC), inverse difference moment (IDM), inertia (INE), cluster shade (CS), cluster prominence (CP), contrast (CON) and dissimilarity (DIS). The equations that allow computing these features are the following:

$$ENE = \sum_{ij} P(i,j)^2 \tag{1}$$

$$ENT = -\sum_{ij} P(i,j) * \log(P(i,j)) \tag{2}$$

$$COR = \frac{\sum_{ij}(i-\mu_x)^*(j-\mu_y)^*P(i,j)}{\frac{\sigma_x}{\sigma_y}} \tag{3}$$

$$HC = \frac{\sum_{ij}((i,j)^*P(i,j)) - (\mu_x{}^*\mu_y)}{\sigma_x{}^*\sigma_y} \tag{4}$$

$$IDM = \sum_{ij} \frac{P(i,j)}{1+(i-j)^2} \tag{5}$$

$$INE = \sum_{ij} (i-j)^2 * P(i,j) \tag{6}$$

$$CS = \sum_{ij} \left((i-\mu_x) + (j-\mu_y)\right)^3 * P(i,j) \tag{7}$$

$$CP = \sum_{ij} \left((i-\mu_x) + (j-\mu_y)\right)^4 * P(i,j) \tag{8}$$

$$CON = \sum_{ij} (i-j)^2 * P(i,j)^2 \tag{9}$$

$$DIS = \sum_{ij} |(i+1) - (j+1)| * P(i,j) \tag{10}$$

The normalized GLCM (*P*) represents the frequency or probability of co-occurrence of gray levels (*i* and *j*) in the image.

These texture statistics are sensitive for some kind of images. In particular, high values of ENE feature is corresponded to uniform regions of the images. ENT feature is equivalent to non-uniform zones of the images. IDM feature implies homogeneity, whereas INE denotes contrast. More details about the semantic means of the features were defined in a previous study (Ávila et al., 2015).

2.2.2.2. One point fractal texture algorithms. OPFTA (Caballero et al., 2017c, 2018a,) is a novelty algorithm based on features obtained from fractal properties values. Initially, the images are divided into smaller rectangles and termed the region of interest (ROI). Then, the local exponents are computed for each ROI, these local exponents reflect the number of times that a pattern is repeated in each ROI depending of the size of boxes that they were calculated in each case. From all local exponent, one of them is selected with the box size equal to eight, since this value is the most representative (Caballero et al., 2017c). After that, one value for each ROI is gathered in order to create a matrix with the fractal values. Each cell of the matrix represents one ROI from the image. Seven features were computed on each matrix. These features were calculated based on second order statistics (Aggarwal and Agrawal, 2012; Peckinpaugh, 1991): uniformity (UNI), ENT, COR, homogeneity (HOM), INE, CON, and efficiency (EFI). The equations to calculate each feature from the values of the previously computed matrix are following indicated:

$$UNI = \sum_i \sum_j P(i,j)^2 \tag{11}$$

$$ENT = \sum_i \sum_j P(i,j) * \log(P(i,j)) \tag{12}$$

$$COR = \frac{\sum_i \sum_j \mu_x{}^*\mu_y{}^*P(i,j)}{\frac{\sigma_x}{\sigma_y}} \tag{13}$$

$$HOM = \sum_i \sum_j \frac{P(i,j)}{1+(i-j)^2} \tag{14}$$

$$INE = \sum_i \sum_j (i-j)^2 * P(i,j) \tag{15}$$

$$CON = \sum_i \sum_j (i-j)^2 * P(i,j)^2 \tag{16}$$

$$EFI = \sum_i \sum_j \frac{\sigma_x}{\mu_x} + \frac{\sigma_y}{\mu_y} \tag{17}$$

Again, *P* (*i,j*) stands for number of times gray tones *i* and *j* have been neighbours.

2.2.3. Prediction equations

Prediction equations obtained by using a predictive techniques of data mining (Multiple Linear Regression, MLR) were selected for the EP. Data mining is an important step of KDD (Knowledge Discovery in Databases), which is mainly related to the non-trivial process of finding knowledge and potentially useful information from data stored in repositories (Fayyad et al., 1996).

The free software WEKA 3.8 (Waikato Environment for Knowledge Analysis) (http://www.cs.waikato.ac. nz/ml/weka/) was used for carrying out the predictive techniques of data mining. The main advantage of the WEKA is that calibration and validation are achieved by using the same data sets, not being necessary to perform the validation with a different data set. This also allows the development of the prediction model. Cross validation of ten folds was used in this study.

2.2.3.1. Multiple linear regression. MLR is used to represent linear relationship between a dependent variable and several independent variables. This technique obtains a linear regression equation, which can be used to predict future values (Hastie et al., 2001). For that, MLR works on a database constructed with the values of the computational features

of MRI and real values of the quality characteristics of the products. This technique steps through the attributes removing the one with the smallest standardized coefficient until no improvement is observed in the estimation of the error. The estimation procedure was 10-fold cross validation (Dietterich, 1998), where the data were divided into 10 partitions of equal size. One subset was tested each time and the remaining data were used for fitting the model. The process was repeated sequentially until all subset were tested. Therefore, all data were used for both training and testing. However, although this method requires ten repetition analysis, this is a robust method (Grossman et al., 2010).

Thus, the equation that define the MLR model is:

$$y = \omega_0 + \sum_i \omega_i x_i, \tag{18}$$

where y is the dependent variable, ω_0 is the y-intercept (constant term), ω_i is the slope coefficients for each explanatory variable, and x_i are the explanatory variables.

Once obtained the equations, they should be made over periodically to assure their accuracy since the database is increasing continuously.

2.3. Evaluation of the experimental protocol

The correlation coefficient (R) is used for evaluating the goodness of the prediction and for its validation.

$$R = \sqrt{\frac{\sum_i (f_i - \overline{y})^2}{\sum_i (y_i - \overline{y})^2}} \tag{19}$$

where fi is the predicted value, yi is the real value and $\overline{y}$ is the average value.

The mean absolute error (MAE) and root mean square error (RMSE) were used to evaluate the prediction results too (Ávila et al., 2019), which measures the difference between real and predicted values. They are given by the following equations:

$$MAE = \frac{1}{n}\sum_i f_i - y_i \tag{20}$$

$$RMSE = \sqrt{\frac{1}{n} * \sum_i (f_i - y_i)^2} * 100 \tag{21}$$

where f_i is the predicted and y_i is the real value.

Real and predicted values were also compared by means of p-value, true standard deviation (TSTD), which evaluates the mean dispersion of the true measurements, and weighted absolute percentage error (WAPE) that measures the mean dispersion of the computer prediction values around the attribute (Ávila et al., 2019)

$$TSTD = \frac{1}{N}\sum_i \sqrt{\frac{1}{M_K - 1} * \sum_j \left(d_{ijk} - \overline{d_{ik}}\right)^2} \tag{22}$$

$$WAPE\ (\%) = \frac{100 \cdot \sum_i |f_i - y_i|}{\sum_i f_i} \tag{23}$$

where f_i and y_i are the predicted and the real values, N is the number of samples, M_K is the number of measurements carried out for each attribute K, d_{ijk} is the jth true measurements of sample i and for the attribute K, while $\overline{d_{ik}}$ is the average over all the measurements for sample i and attribute K.

2.4. PHYSICO-CHEMICAL and sensory analysis

The physico-chemical analysis carried out in the loins of this study were: moisture (determined at 102 ± 2 °C by the official method (A.O.A.C., 2000; reference 935.29)), lipid content (determined gravimetrically with chloroform/methanol (2:1, v/v), according to the method described in Perez-Palacios et al. (2008)); water activity (with the system Lab Master-aw (NOVASINA AG, Switzerland) that was calibrated at 20–22 °C before use), instrumental color (with a Minolta CR-300 colorimeter (Minolta Camera Corp., Meter Division, Ramsey, NJ, determining lightness (L), redness (a^*), and yellowness (b^*), and standardized before use with a white tile). Salt content was determined volumetrically in dry-cured loins by the official method (A.O.A.C., 2000; reference 971.19). All determinations were done in triplicate.

The sensory analysis of the dry-cured loins was assessed by a trained panel of thirteen members using quantitative-descriptive analysis (Ruiz et al., 1998). Eleven traits of Iberian dry-cured loins (redness of lean, brightness of lean, marbling, odour intensity, hardness, juiciness, salty taste, flavor intensity, cured flavor, rancid flavor and flavor persistence) were assessed on a non-structured scale of 0–10. Analyses were performed in tasting rooms with the conditions specified in the UNE-EN ISO 8589:2010 regulations. All sessions were conducted at room temperature (22 °C) in rooms equipped with white fluorescent lighting (220–230 V, 35 W). The software used to record the scores in the sensory sessions was FIZZ Network (version 2.20, Biosystems, France). For each loin, two slices (1.5 mm) were given to the panellists. Slices were obtained using a commercial slicing machine and were served to the panellists on plates at room temperature. The panel sessions were held mid-morning, approximately 4 h after breakfast. Three samples randomly presented to the panellist were analysed in each session. Approximately 200 ml of water at room temperature was provided to the panellists. During each session, the panel average for each sample was recorded.

3. Results and discussion

3.1. Selection of the optimum procedures

Different LF MRI studies on pork loins (Caballero et al., 2017a,b; 2018a,b; Pérez-Palacios et al., 2017) have been evaluated in the present work, by comparing prediction results on physico-chemical and sensory characteristics as a function of the acquisition sequences of MRI, algorithms for the image analysis and techniques of data analysis. Three acquisition sequences have been used in the LF MRI studies in pork loin: SE, GE and T3D. In general, SE led to sharper and better-defined images than GE and T3D (Caballero et al., 2017a,b; 2018a,b) and the best prediction results (Caballero et al., 2017a,b; 2018a,b).

Algorithms to analyse MRI differ in the number of computational features and complexities. NGLDM is the simplest algorithm, with 5 computational features, following in increasing order by OPFTA (7), CFA (9) and FTA, GLCM and GLRLM (10). As for the complexity, it is lower in GLCM, GLRLM and OPFTA (O (n^2)) than in FTA (O ($n^2 * \log n$)) and NGLDM and CFA (O (n^3)) (Caballero et al., 2018a). Considering the results on prediction of the physico-chemical and sensory characteristics, GLCM and OPFTA achieved the highest correlation coefficients among the texture and fractal algorithms, respectively (Caballero et al., 2017a,b; 2018a,b; Pérez-Palacios et al., 2017). Thus, instead of not being the simplest algorithms, GLCM and OPFTA were selected for the EP.

MLR and Isotonic Regression (IR) have been tested as predictive techniques in the LF MRI studies on pork loins. In the case of applying texture algorithms for the image analysis, excellent correlation coefficients (R > 0.75) were achieved with both MLR and IR (Caballero et al., 2017b; Pérez-Palacios et al., 2017). However, more accurate prediction results were obtained with MLR than with IR when using fractal algorithms (Caballero et al., 2017a, 2018a,b). The MAE was also calculated in these studies, being lower when using MLR in both cases (texture and fractal algorithms). Besides, MLR is simpler (first degree equation) than IR (sixth degree equations) (Caballero et al., 2017a,b; 2018a,b; Pérez-Palacios et al., 2017). Accordingly, prediction equations

Table 1
Prediction equations (as a function of the computational features of GLCM or OPFTA) of the quality parameters of loins, obtained by Multiple Linear Regression and used in the experimental protocol.

		GLCM		OPFTA	
a_w		=- 0.034 * ENE +0.012 * ENT – 0.059 * COR +0.974 * HC + 0.073 * IDM +0.197 * INE – 0.070 * CS – 0.036 * CP + 0.063 * CON – 0.295 * DIS +0.919	(24)	= 0.368 * UNI + 0.334 * ENT + 0.020 * COR + 0.025 * HOM + 0.162 * INE – 0.135 * CON + 0.145 * EFI + 0.566	(25)
Moisture (%)		= - 11.038 * ENE + 6.316 * ENT – 7.109 * COR + 24.830 * HC + 24.389 * IDM + 55.696 * INE – 20.659 * CS – 15.407 * CP + 10.157 * CON – 70.601 * DIS + 45.927	(26)	= 49.568 * UNI + 64.839 * ENT + 4.683 * COR + 16.969 * HOM + 55.767 * INE – 30.923 * CON + 42.805 * EFI – 25.929	(27)
Instrumental color	L*	= - 6.759 * ENT – 16.836 * COR + 25.396 * HC + 0.964 * IDM + 28.971 * INE – 5.108 * CS + 2.132 * CP – 16.028 * CON – 31.809 * DIS + 47.607	(28)	= 14.892 * ENT + 18.902 * HOM + 31.617 * INE – 29.366 * CON + 19.365 * EFI + 26.536	(29)
	a	= 2.223 * ENE – 2.416 * ENT + 1.514 * COR + 1.282 * HC – 3.919 * IDM + 9.143 * INE + 2.848 * CS – 4.142 * CON + 10.490 * DIS + 13.516	(30)	= - 2.950 * HOM – 7.324 * INE + 7.488 * CON – 6.859 * EFI + 15.579	(31)
	b	= 2.311 * ENE – 0.763 * ENT + 0.916 * HC – 1.620 * IDM – 4.527 * INE + 1.991 * CS + 6.770 * CP + 7.878 * CON + 11.325 * DIS + 4.256	(32)	= 12.883 * UNI + 3.205 * ENT – 4.705 * HOM – 6.591 * INE – 7.734 * EFI + 5.644	(33)
Salt content (%)		= 1.838 * COR – 2.226 * HC – 1.037 * IDM – 6.009 * INE + 1.574 * CS + 1.344 * CP + 7.336 * DIS + 0.821	(34)	= - 8.898 * UNI – 7.546 * ENT – 0.506 * COR – 0.265 * HOM – 3.655 * INE + 3.281 * CON – 3.224 * EFI + 9.312	(35)
Lipid content (%)		= 11.641 * ENE – 10.390 * ENT + 7.151 * HC – 16.961 * IDM – 22.839 * INE + 8.873 * CS + 12.602 * CP – 22.772 * CON + 27.982 * DIS + 17.497	(36)	= - 15.617 * ENT – 7.474 * HOM – 13.201 * INE – 22.415 * EFI + 36.191	(37)
Redness of lean		= 1.784 * ENT – 2.828 * HC + 8.185 * IDM – 3.981 * INE + 3.855 * CP + 2.916 * CON + 5.247 * DIS + 3.805	(38)	= 4.403 * ENT – 1.131 * COR + 0.826 * HOM – 1.253 * INE + 1.711 * CON + 5.137 * EFI + 3.062	(39)
Brightness of lean		= 0.323 * ENT + 28.978 * COR + 1.917 * HC – 2.781 * IDM – 2.385 * INE + 4.523 * CP – 1.302 * CON + 3.328 * DIS + 2.657	(40)	= 2.616 * UNI – 0.754 * INE – 6.529 * EFI + 4.764	(41)
Marbling of lean		= - 3.966 * ENT + 6.765 * HC – 19.609 * IDM + 5.838 * INE – 3.113 * CP – 4.309 * CON – 12.017 * DIS + 13.324	(42)	= 3.262 * UNI – 8.596 * ENT + 2.673 * COR – 1.556 * HOM + 1.797 * INE – 5.698 * CON – 11.163 * EFI + 14.636	(43)
Odour intensity		= 38.889 * COR + 2.050 * HC – 3.797 * IDM + 2.473 * CP – 4.119 * CON + 3.563 * DIS + 5.346	(44)	= - 1.657 * ENT + 0.689 * COR + 0.703 * HOM – 0.596 * INE + 0.792 * CON – 7.707 * EFI + 8.223	(45)
Hardness of lean		= - 1.535 * ENE + 2.435 * ENT – 3.284 * HC + 9.761 * IDM – 2.479 * INE + 0.405 * CS + 2.030 * CP + 8.202 * DIS + 1.065	(46)	= - 2.218 * UNI + 3.948 * ENT – 1.231 * COR + 1.130 * HOM – 1.128 * INE + 3.647 * CON + 3.244 * EFI + 1.675	(47)
Juiciness		= - 1.321 * ENT + 3.156 * HC – 7.674 * IDM – 1.028 * CON – 3.026 * DIS + 7.570	(48)	= 1.008 * UNI – 3.229 * ENT + 1.176 * COR – 1.511 * CON – 5.796 * EFI + 8.809	(49)
Salty taste		= 0.507 * ENT + 22.855 * COR + 1.606 * HC – 5.033 * INE + 5.735 * CP + 1.421 * CON + 4.014 * DIS + 2.307	(50)	= 4.354 * UNI + 2.113 * ENT – 1.231 * INE – 5.437 * EFI + 3.312	(51)
Flavor intensity		= - 1.533 * ENE + 0.201 * ENT + 21.101 * COR + 1.424 * HC – 1.022 * IDM – 2.309 * INE + 2.129 * CP – 0.371 * CON + 2.901 * DIS + 5.203	(52)	= 1.513 * UNI – 5.347 * EFI + 6.761	(53)
Flavor persistence		= - 2.047 * ENE + 0.395 * ENT + 22.681 * COR + 1.174 * HC – 2.458 * INE + 1.807 * CP – 0.553 * CON + 3.881 * DIS + 3.788	(54)	= 0.844 * UNI + 0.630 * CON – 5.164 * EFI + 5.698	(55)
Cured flavor		= 0.774 * ENT + 24.530 * COR + 0.887 * HC – 2.660 * INE + 5.047 * CP – 1.733 * CON + 5.183 * DIS + 3.401	(56)	= 1.143 * HOM – 0.501 * INE – 4.126 * EFI + 6.135	(57)
Rancid flavor		= 1.110 * ENE + 0.630 * ENT – 0.996 * HC + 2.124 * IDM – 1.113 * INE + 2.285 * CP + 0.788 * CON + 1.393 * DIS + 0.763	(58)	= 0.487 * UNI + 1.506 * ENT – 0.320 * COR + 0.386 * HOM – 0.595 * INE + 2.156 * EFI + 0.477	(59)

obtained by MLR were selected for the EP.

3.2. Implementation and validation the experimental protocol

Considering the above comparison work, the EP was implemented with two procedures: SE – GLCM – prediction equations obtained by MLR as a function of computational texture features of GLCM and SE – OPFTA - prediction equations obtained by MLR as a function of computational fractal features of OPFTA (Fig. 1B). Table 1 shows the prediction equations of the EP for both procedures. Once the EP was accomplished with the two optimum procedures, it was performed

Table 2
Quality measures of the prediction procedures (with GLCM or OPFTA) of the experimental protocol: correlation coefficient (R), weighted absolute percentage error (WAPE) and root mean square error of prediction (RMSEP).

		GLCM			OPFTA		
		R	WAPE	RMSEP	R	WAPE	RMSEP
a_w		0.6747	0.010	0.009	0.8491	0.011	0.010
Moisture (%)		0.9114	0.050	0.205	0.8789	0.050	0.204
Instrumental color	L*	0.9076	0.181	0.181	0.9017	0.175	0.175
	a	0.6123	0.060	0.060	0.6961	0.041	0.041
	b	0.7064	0.096	0.096	0.8511	0.049	0.049
Salt content (%)		0.8909	0.094	0.024	0.8905	0.080	0.021
Lipids content (%)		0.8388	0.102	0.110	0.8489	0.073	0.079
Redness of lean		0.5697	0.076	0.048	0.6491	0.048	0.041
Brightness of lean		0.9471	0.123	0.079	0.9270	0.093	0.059
Marbling of lean		0.9097	0.123	0.081	0.9257	0.095	0.062
Odour intensity		0.9588	0.135	0.079	0.9591	0.114	0.067
Hardness of lean		0.7477	0.108	0.065	0.9183	0.073	0.044
Juiciness		0.7692	0.108	0.054	0.9249	0.075	0.037
Salty taste		0.9560	0.124	0.059	0.9513	0.087	0.041
Flavor intensity		0.9442	0.067	0.048	0.9791	0.042	0.030
Flavor persistence		0.9259	0.076	0.058	0.9764	0.042	0.032
Cured flavor		0.9491	0.097	0.055	0.9777	0.063	0.036
Rancid flavor		0.8588	0.181	0.032	0.9137	0.146	0.026

Table 3
Comparison between physico-chemical (P–C) and predicted results from the GLCM and OPFTA procedures of the experimental protocol[a].

		P–C	GLCM	OPFTA	*p* (P–C vs GLCM)	*p* (P–C vs OPFTA)
a_w		0.875 ± 0.009	0.875 ± 0.011	0.879 ± 0.016	0.557	0.068
Moisture (%)		40.119 ± 3.407	39.394 ± 4.381	40.976 ± 3.537	0.182	0.075
Instrumental color	*L*	45.179 ± 3.148	45.036 ± 3.973	45.753 ± 3.478	0.772	0.211
	a[a]	14.705 ± 0.576	14.329 ± 0.537	14.821 ± 0.294	0.316	0.067
	b[a]	8.713 ± 0.557	9.402 ± 1.093	8.502 ± 0.699	0.752	0.209
Salt content (%)		2.503 ± 0.385	2.431 ± 0.447	2.480 ± 0.409	0.211	0.604
Lipid content (%)		10.580 ± 1.198	11.257 ± 1.569	10.027 ± 0.867	0.362	0.707

[a] Values are expresses as mean ± standard deviation; *p*-value < 0.05 indicates significant differences.

within the official analysis service of the Faculty of Veterinary Science at University of Extremadura (Cáceres, Spain) and evaluated with real samples, as explained in the experimental design subsection (Fig. 1B).

Table 2 shows values for R, WAPE and RMSE that evaluate the prediction results of the two procedures of the EP (by using GLCM or OPFTA). R values are higher than 0.75 for most quality parameters of loins, which indicates a very good to excellent correlation (Colton, 1974), when applying both GLCM and OPFTA. Besides, the WAPE and the RMSE are lower than 0.02% and 0.3%, respectively, in all the cases. Instead of the adequacy of these quality measures for both procedures, it can be observed a higher number of predicted parameters with $R > 0.75$ and WAPE <0.01 when using OPFTA. This fact shows the suitability of these optimized procedures in the EP.

Giving a step forward, results from physico-chemical and sensory analyses have been statistically compared with those predicted by GLCM and OPFTA procedures. Mean values and standard deviation of physico-chemical and sensory parameters from traditional analyses and predicted by GLCM and OPFTA procedures are shown in Table 3 and Fig. 2, respectively, which also expose the *p*-values between real and predicted values. No significant differences ($p > 0.05$) were found between real and predicted results in all cases. It is also noted in Table 3 and Fig. 2, some differences in the standard deviation of the results, being, overall, higher in the GLCM predicted values than in the real and OPFTA predicted.

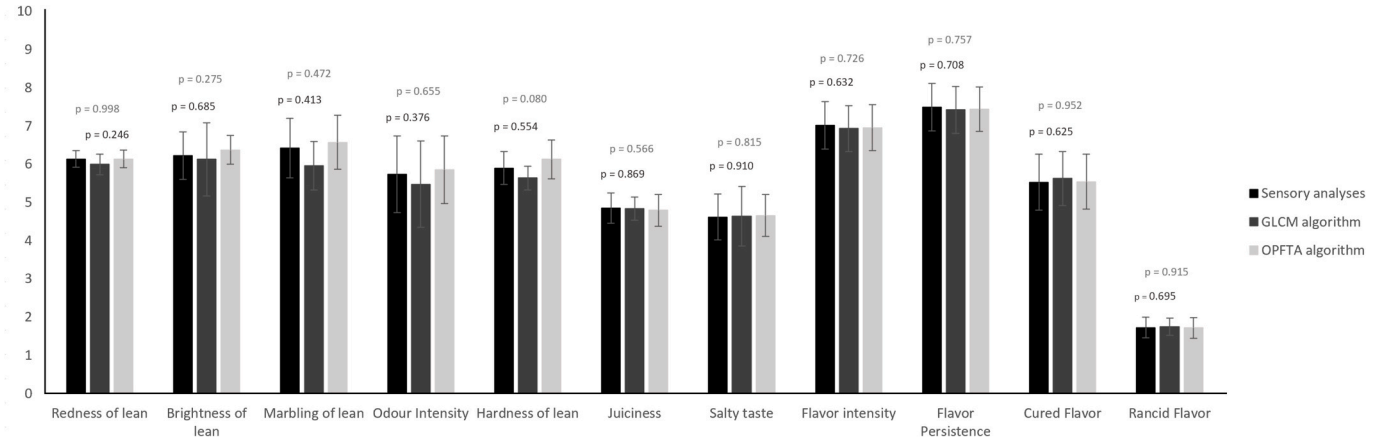

Fig. 2. Mean values (columns), standard deviation (error bars) and p-values between values real and GLCM predicted (dark grey) and real and OPFTA predicted (light grey) of the loin attributes obtained from the sensory analysis and predicted by the GLCM and OPFTA procedures of the experimental protocol.

Table 4
Dispersion of the results from the physico-chemical and sensory analysis (Mean Absolute Error, MAE) and predicted by GLCM and OPFTA (True Standard Deviation, TSTD).

		TSTD	MAE	
			GLCM	OPFTA
a_w		0.014	0.009	0.010
Moisture (%)		3.913	1.998	1.995
Instrumental color	*L*	3.611	0.039	0.038
	*a**	0.760	0.040	0.027
	*b**	0.684	0.107	0.055
Salt content (%)		0.4453	0.236	0.201
Lipids content (%)		1.4671	1.075	0.776
Redness of lean		0.5443	0.468	0.400
Brightness of lean		1.4465	0.767	0.576
Marbling of lean		1.7544	0.788	0.610
Odour intensity		2.1552	0.773	0.656
Hardness of lean		0.9234	0.638	0.432
Juiciness		0.9012	0.523	0.363
Salty taste		1.3192	0.574	0.402
Flavor intensity		1.3212	0.472	0.294
Flavor persistence		1.3352	0.568	0.316
Cured flavor		1.5853	0.538	0.352
Rancid flavor		0.6585	0.312	0.251

In view of this fact, TSTD and MAE were measured (Table 4). The TSTD evaluates the mean dispersion of the true measurements, and MAE evaluates the mean dispersion of the predicted values around the characteristics, which is the average over the true measurements. In all quality parameters, TSTD values are higher than MAE of GLCM and OPFTA procedures, indicating a lower dispersion in the computer prediction than in the true measurements. This finding was also shown by Ávila et al. (2019), which ascribed to the low number of measurements for the physico-chemical and sensory characteristics. This aspect may also influence in the results of the present study since each sample (n = 100) was evaluated in triplicate by means of physico-chemical and sensory analysis, while twenty-nine MRI images are obtained and computationally analysed for each loin. It is also observed in Table 4, slightly higher MAE values for quality parameters predicted by GLCM than by OPFTA. This finding corroborates the values of R, WAPE and RMSE (Table 2) previously discussed and may be affected by the relationship between the quality parameters of loins and the computational features.

5. Conclusions

An experimental protocol has been developed for the non-destructive analysis of quality parameters of meat products by MRI-computer vision-data mining. The comparison of different techniques for the MRI acquisition, the MRI analysis and the data analysis to predict quality parameters of pork loins have led to two optimum procedures (SE – GLCM – prediction equations obtained by MLR as a function of computational texture features of GLCM and SE – OPFTA - prediction equations obtained by MLR as a function of computational fractal features of OPFTA) to be implemented in an experimental protocol. The validation of these two procedures in a high number of samples from the meat industry by several quality measures allows to indicate the use of any of them to determine quality characteristics of loins by LF MRI in a non-destructive way, with high accuracy and reducing the dispersion of the values. These results bring the possibility of implementing this methodology in meat processing plants. For that, some improvements in the image acquisition (time reduction) and image and data analysis (software development to provide on-line results) should be done.

Author contributions

DANIEL CABALLERO, Conceptualization; Formal analysis; Funding acquisition; Investigation; Methodology; Software; Validation; Visualization; Writing – original draft. PABLO G. RODRÍGUEZ, Conceptualization; Funding acquisition; Investigation; Methodology; Supervision. ANDRÉS CARO, Data curation; Formal analysis; Funding acquisition; Investigation; Methodology; Project administration; Supervision; Validation; Visualization; Writing – review & editing. MARÍA DEL MAR ÁVILA, Data curation; Formal analysis; Funding acquisition; Investigation; Methodology; Project administration; Supervision; Validation; Visualization; Writing – review & editing. JUAN P. TORRES, Formal analysis; Methodology; Software. TERESA ANTEQUERA, Formal analysis; Funding acquisition; Investigation; Methodology; Resources; Supervision; Validation; Writing – original draft; Writing – review & editing. TRINIDAD PÉREZ-PALACIOS, Conceptualization; Formal analysis; Funding acquisition; Investigation; Methodology; Resources; Supervision; Validation; Visualization; Writing – original draft; Writing – review & editing.

Declaration of competing interest

All authors have participated in (a) conception and design, or analysis and interpretation of the data; (b) drafting the article or revising it critically for important intellectual content; and (c) approval of the final version.

Acknowledgments

Daniel Caballero thanks the “Junta de Extremadura” for the postdoctoral grant (PO17017). The authors wish to acknowledge the funding received from the FEDER-MICCIN Infrastructure Research Project (UNEX-10-1E-402), Junta de Extremadura economic support for research group (GRU18138 and GRU18104) and for the Regional Government Board – Research Project (IB16089). We also wish to thank the Animal Source Foodstuffs Innovation Services (SiPA) (Cáceres, Spain) from the University of Extremadura.

References

Aggarwal, N., Agrawal, R.K., 2012. First and second order statistics features for classification of magnetic resonance brain images. J. Signal Inf. Process. 3, 574–850.
Association of Official Analytical Chemists (A.O.A.C.), 2000. In: Official Methods of Analysis of AOAC International, vols. 1 and 2. AOAC International, Gaithersburg, Maryland, U.S.A.
Ávila, M.M., Caballero, D., Durán, M.L., Caro, A., Pérez-Palacios, T., Antequera, T., 2015. Including 3D-textures in a computer vision system to analyze quality traits of loin. Lect. Notes Comput. Sci. 9163, 456–465.
Ávila, M.M., Caballero, D., Antequera, T., Durán, M.L., Caro, A., Pérez-Palacios, T., 2018. Applying 3D textura algorithms on MRI to evaluate quality traits of loin. J. Food Eng. 222, 258–266.
Ávila, M.M., Durán, M.L., Caballero, D., Antequera, T., Pérez-Palacios, T., Cernadas, E., Fernández-Delgado, M., 2019. Magnetic Resonance Imaging, texture analysis and regression techniques to non-destructively predict the quality characteristics of meat pieces. Eng. Appl. Artif. Intell. 82, 110–125.
Bernau, M., Kremer, P.V., Lauterbach, E., Tholen, E., Petersen, B., Pappenberger, E., Scholz, A.M., 2015. Evaluaton of carcass composition of intact boars using linear measurements from performance testing, dissection, dual energy X-ray absorptiometry (DXA) and magnetic resonance imaging (MRI). Meat Sci. 104, 58–66.
Caballero, D., Pérez-Palacios, T., Caro, A., Amigo, J.M., Dahl, A.B., Ersboll, B.K., Antequera, T., 2017a. Prediction of pork quality parameters by applying fractals and data mining on MRI. Food Res. Int. 99, 739–747.
Caballero, D., Antequera, T., Caro, A., Ávila, M.M., Rodríguez, P.G., Pérez-Palacios, T., 2017b. Non-destructive analysis of sensory traits of dry-cured loins by MRI-computer vision techniques and data mining. J. Sci. Food Agric. 97, 2942–2952.
Caballero, D., Caro, A., Amigo, J.M., Dahl, A.B., Ersboll, B.K., Pérez-Palacios, T., 2017c. Development of a new fractal algorithm to predict quality traits of MRI loins. Lect. Notes Comput. Sci. 10424, 208–218.
Caballero, D., Caro, A., Dahl, A.B., Ersboll, B.K., Amigo, J.M., Pérez-Palacios, T., Antequera, T., 2018a. Comparison of different image analysis algorithms on MRI to predict physico-chemical and sensory attributes of loin. Chemometr. Intell. Lab. Syst. 180, 54–63.
Caballero, D., Antequera, T., Caro, A., Amigo, J.M., Ersboll, B.K., Dahl, A.B., Pérez-Palacios, T., 2018b. Analysis of MRI by fractals for Prediction of sensory attributes: a case of study in loin. J. Food Eng. 227, 1–10.
Caballero, D., Pérez-Palacios, T., Caro, A., Antequera, T., 2021. Use of Magnetic Resonance Imaging to analyse meat and meat products non-destructively. Food Rev. Int. https://doi.org/10.1080/87559129.2021.1912085.

Colton, T., 1974. Statistical in Medicine. Little Brown and Co., New York, New York, U.S. A, pp. 1–372.
Dietterich, T., 1998. Approximate statistical tests for comparing supervised classification learning algorithms. Neural Comput. 10 (7), 1895–1923.
Fayyad, U., Piatetsky-Shapiro, L.G., Smyth, P., 1996. From data mining to knowledge discovery in databases. Am. Ass. Artifi. Intel. 17, 37–54.
Feig, S., 2011. Comparison of costs and benefits of breast cancer screening with mammography, ultrasonography, and MRI. Obstet. Gynecol. Clin. N. Am. 38 (1), 179–196.
González-Mohino, A., Antequera, T., Ventanas, S., Caballero, D., Mir-Bel, J., Pérez-Palacios, T., 2018. Near-infrared spectroscopy-based analysis to study sensory parameters on pork loins as affected by cooking methods and conditions. J. Sci. Food Agric. 98, 4227–4236.
Grossman, R., Seni, G., Elder, J., Agarwal, N., Liu, H., 2010. Ensemble methods in data mining: improving accuracy through combining predictions. Synthesis lectures on data mining and knowledge discovery 2 (1), 1–126.
Haralick, R.M., Shanmugam, K., Dinstein, I., 1973. Textural features for image classification. IEEE Trans. Syst. Man Cyber. 3 (6), 610–621.
Haralick, R.M., Shapiro, L.G., 1993. Computer and Robot Vision. Addison-Wesley, Chicago, Illinois, U.S.A, pp. 453–508.
Hastie, T., Tibshirani, R., Friedman, J., 2001. The Elements of Statistical Learning: Data Mining Inference and Prediction. Springer-Verlag, New York, New York, U.S.A, pp. 43–100.
Ladd, M.E., Bachert, P., Meyerspeer, M., Moser, E., Nagel, A.M., Norris, D.G., Schmitter, S., Speck, O., Straub, S., Zaiss, M., 2018. Pros and cons of ultra-high-field MRI/MRS for human application. Prog. Nucl. Magn. Reson. Spectrosc. 109, 1–50.
Molano, R., Rodríguez, P.G., Caro, A., Durán, M.L., 2012. Finding the largest area rectangle of arbitrary orientation in a closed contour. Appl. Math. Comput. 218 (19), 9866–9874.
Peckinpaugh, S., 1991. An improved method for computing gray-level co-occurrence matrix based texture measured. Comput. Vis. Graph Image Process 53, 574–580.
Pérez-Palacios, T., Ruiz, J., Martín, D., Muriel, E., Antequera, T., 2008. Comparison of different methods for total lipid quantification. Food Chem. 110, 1025–1029.
Pérez-Palacios, T., Antequera, T., Durán, M.L., Caro, A., Rodríguez, P.G., Ruiz, J., 2010a. MRI-based analysis, lipid composition and sensory traits for studying Iberian dry-cured hams from pigs fed with different diets. Food Res. Int. 43, 248–254.
Pérez-Palacios, T., Antequera, T., Molano, R., Rodríguez, P.G., Palacios, R., 2010b. Sensory traits Prediction in dry-cured hams from fresh product via MRI and lipid composition. J. Food Eng. 101, 152–157.
Pérez-Palacios, T., Caballero, D., Antequera, T., Durán, M.L., Ávila, M.M., Caro, A., 2017. Optimization of MRI acquisition and texture analysis to predict physico-chemical parameters of loins by data mining. Food Bioprocess Technol. 10, 750–758.
Pérez-Palacios, T., Caballero, D., González-Mohino, A., Mir-Bel, J., Antequera, T., 2019. Near infrared reflectance spectroscopy to analyse texture related characteristics of sous vide pork loin. J. Food Eng. 263, 417–423.
Picouet, P.A., Gou, P., Fulladosa, E., Santos-Garcés, E., Arnau, J., 2013. Estimation of NaCl diffusivity by computed tomography in the semimembranosus muscle during salting of fresh and frozen/thawed hams. LWT Food Sci. Technol. 51, 275–280.
Ruiz, J., Ventanas, J., Cava, R., Timón, M.L., García, C., 1998. Sensory characteristics of Iberian ham: influence of processing time and slice location. Food Res. Int. 31, 53–58.
Torres, J.P., Ávila, M.M., Caro, A., Pérez-Palacios, T., Caballero, D., 2019. Non-destructively Prediction of quality parameters of dry-cured Iberian ham by applying Computer vision and low-field MRI. Lect. Notes Comput. Sci. 11867, 498–507.
Vestergaard, C., Erbou, S.G., Thauland, T., Adler-Nissen, J., Berg, B., 2015. Salt distribution in dry-cured ham measured by computed tomography and image analysis. Meat Sci. 69, 9–15.